HU-TFT-95-47, DUKE-TH-95-96, LBL-37642

Screening of initial parton production in ultrarelativistic heavy-ion collisions

K. J. Eskola

Laboratory of High Energy Physics and Research Institute for Theoretical Physics, P.O. Box 9, FIN-00014 University of Helsinki, Finland

B. Müller

Department of Physics, Duke University, Durham, NC 27708-0305, U.S.A.

Xin-Nian Wang

Nuclear Science Division, MS 70A-3307, Lawrence Berkeley Laboratory, University of California, Berkeley, CA 94720, U.S.A.

(August, 1995)

Abstract

Screening of initial parton production due to the presence of on-shell partons in high-energy heavy-ion collisions is discussed. It is shown that the divergent cross sections in the calculation of parton production can be regulated self-consistently without an *ad hoc* cut-off, and that the resultant parton production and transverse energy production rate are finite. Consequences on the energy density estimates are discussed.

PACS numbers:12.38.Mh,25.75+r,12.38.Bx

Hard and semihard parton scatterings have been shown to play an important role in both high energy $pp(\bar{p})$ and ultrarelativistic heavy ion collisions. In $pp(\bar{p})$ collisions they are believed to be responsible for the rapid growth of the inelastic and total cross sections [1,2], and in AA collisions they are expected to produce a large amount of transverse energy in the central rapidity region [3–6]. Because the dominant QCD parton cross sections are singular in the soft scattering limit, most model calculations of minijet production via perturbative QCD (pQCD) have introduced an infrared cut-off, p_0, corresponding to the smallest permissible transverse momentum transfer in a $2 \to 2$ parton scattering, to which perturbative QCD can still be applied. This cut-off is used in most of the models to separate perturbative hard processes from nonperturbative soft interactions which can be modeled, e.g., by strings or flux tubes. Since there is no distinct boundary between soft and hard physics, both the hard and soft part of the interaction in this scheme are very sensitive to the cut-off p_0.

Heavy ion collisions differ from pp collisions in that minijets are produced in large number, so that a medium of minijets is formed. In the space-time evolution of a heavy-ion collision soft particle production will be completed after semihard and hard processes. Therefore, the soft interactions are expected to be screened by interactions with the semihard quanta (minijets). We here take a step further by proposing that the perturbative semihard particle production should also be screened by the processes which have happened even earlier, i.e., by the harder processes. In this paper we will study the influence of the final-state interactions among minijets. We will investigate to what extent minijet production is screened and whether the screening effect can provide an effective self-consistent regularization of the infrared behavior of minijet production.

Consider an example of two hard processes as illustrated in Fig. 1. Let us assume jets from the first hard scattering are produced in the 90 degree direction and have a large transverse momentum p_{T1}. Because of this large transverse momentum, the interaction point is well localized in the transverse direction to a distance of $1/p_{T1}$. As these two jets travel in the transverse direction, they will experience secondary interactions. These secondary interactions can give rise to many nuclear effects of hard scatterings, i.e., energy loss and Cronin effects. Since we are interested in the screening effects caused by these final state interactions, we will consider the interactions of the produced hard partons with the propagating parton in another scattering nearby as shown in Fig. 1. A semiclassical estimate of the screening requires that different scattering events can be treated as incoherent. We will show that this condition is satisfied if the produced partons, which screen other softer interactions, can be treated as on-shell particles.

In a parton model, we treat partons from the nuclei and out-going partons as on-shell. Therefore, the propagator in the first hard scattering must be off-shell by $-p_{T1}^2$. One notices that there is one extra loop in the Feyman diagram in Fig. 1 as compared to that of two independent scatterings. The loop-momentum integration will then

put one of the propagators on shell. Since we demand that the second scattering also has transverse momentum transfer p_{T2}, the propagators in this scattering will also be off-shell by $-p_{T2}^2$. Therefore, the dominant contribution to the loop-momentum integration comes from the pole of the propagator between the two scatterings in which the propagating parton will be put on-shell. The condition for this contribution to be dominant is that the distance $\Delta x_\perp$ between the two scatterings must be larger than the interaction range of the two hard scatterings which are determined by the off-shellness of the exchanged gluons, i.e., $\Delta x_\perp > \max(1/p_{T1}, 1/p_{T2})$. If this condition is not satisfied, the propagating parton between two scatterings cannot be treated as real and consequently one cannot treat the multiple scatterings as incoherent scatterings. One can thus consider

$$\tau_f(p_T) = \frac{a}{p_T} \tag{1}$$

as the formation time of the produced parton in the mid-rapidity from the hard or semihard scatterings after which they can be treated as real (on-shell) particles and can screen other interactions with smaller transverse momentum transfer. Here we used a dimensionless coefficient a of the order unity to characterize the uncertainty in the formation time.

Let us visualize high-energy AA collisions as in Fig. 2. In this idealized space-time picture the incoming nuclei are very thin slabs, the primary semihard parton-parton collisions all start at $t = 0$ and the forming system at central rapidity is longitudinally boost invariant. In the space-time evolution of the collision the partons with larger p_T are produced earlier, as implied by Eq. 1. These hard partons will then screen production of partons with smaller p_T later in time and space. For the central region around $y = 0$, we will consider the screening effect of partons within a unit rapidity interval, $\Delta y = Y = 1$. We assume minijets have a plateau in the rapidity distribution, which is a good approximation both at LHC and RHIC energies for our choice of Y. For a fixed p_T, partons with larger rapidities form later in our given frame, along the proper time hyperbola as in Fig. 2. In this picture, the formed partons can therefore only screen those scatterings which are in the same rapidity region.

Following Ref. [7], we can estimate the static electric screening mass generated by the produced minijets. The number distribution of minijets produced in an AA collision at an impact parameter $\mathbf{b} = \mathbf{0}$ can be written as [4]

$$\frac{dN_{AA}}{dp_T^2 dy} = T_{AA}(\mathbf{0}) \frac{d\sigma_{jet}}{dp_T^2 dy}, \tag{2}$$

where $T_{AA}(\mathbf{b})$ is the nuclear overlap function and

$$\frac{d\sigma_{jet}}{dp_T^2 dy} = K \sum_{\substack{ijkl= \\ q,\bar{q},g}} \int dy_2 x_1 f_i(x_1, p_T^2) x_2 f_j(x_2, p_T^2) \frac{d\hat{\sigma}^{ij\to kl}}{d\hat{t}}(\hat{s}, \hat{t}, \hat{u}) \tag{3}$$

is the minijet cross section. The hats refer to the partonic sub-processes, x_i is the momentum fraction of the initial state parton i, p_T is the transverse momentum, y_k is the rapidity of the final state parton k, f_i is the parton distribution function, and $K = 2$ is a factor simulating the contribution from the $\mathcal{O}(\alpha_s^3)$ terms in the cross section [8,9]. In what follows, we will compute the minijet production from the complete lowest order formula in Eq. 3 but will finally treat all the minijets as gluons. This should again be a good approximation, since gluons clearly dominate the minijet production at these energies and transverse momenta [10].

To obtain an estimate of the average parton number density in the central region at a given time τ_f, we divide Eq. 2 by the approximate volume $V = \pi R_A^2 \Delta z \approx \pi R_A^2 \tau_f \Delta y$ of the produced system. Then the screening mass from Ref. [7] becomes

$$\mu_D^2(p_T) \approx \frac{3\alpha_{\rm s}}{R_A^2 \tau_f(p_T) Y} 2\arcsin[\tanh(Y/2)] \int_{p_T}^{\sqrt{s}/2} dk_T \frac{dN_{AA}}{dk_T^2 dy}\bigg|_{y=0}. \qquad (4)$$

At this point there are several remarks to be made. First, as done in Ref. [7], we have replaced the thermal (isotropic) Bose-Einstein distribution by the non-isotropic minijet distribution, and assumed that the screening mass can still be calculated from the equilibrium formula given in [7].

Second, note that the lower limit in the k_T-integration in Eq. 4 is p_T. In this way, we are considering a maximal screening effect by assuming that all the quanta with transverse momenta $k_T \geq p_T = a/\tau$ screen the formation of partons at transverse momenta $k_T < p_T$. Also, as explained in the previous paragraphs, only the quanta within the rapidity window Y are assumed to contribute to the screening mass. However, from Eq. 4 we see that as far as the interval Y is small enough, the screening mass is almost independent of the choice for Y, due to the division by the volume of the system. Finally, the scale choice for the running coupling is not clear. Here we just use the p_T of the primary semihard processes.

As we know from studies of pQCD at finite temperature, perturbation theory does not generate static screening in the magnetic part of interactions [11,12]. One normally has to introduce a nonperturbative magnetic mass to regulate the infrared singularities in the transverse part of a gluon propagator. Since the magnetic screening mass in the static limit is not known, let us proceed in the following phenomenological way to get an order of magnitude estimate on the screening effects. We will use the computed electric screening mass as a regulator for the divergent $\hat{t}$- and $\hat{u}$-channel sub-processes. We will simply make a replacement $-\hat{t}(\hat{u}) \rightarrow -\hat{t}(\hat{u}) + \mu_D^2$ in the minijet cross section of Eq. 3. Since the $\hat{s}$-channel processes are not important here, we do not need to make the above replacement for $\hat{s}$. Then we are also safe from the contradiction that the invariant $\hat{s}$ is always positive but the screening mass μ_D is computed for a spacelike gluon.

In Fig. 3 we show the screening mass μ_D and the screened one-jet cross section as functions of p_T. In the upper panel the results are shown for the LHC energy (per

nucleon pair) $\sqrt{s} = 5.5$ TeV and in the lower panel for the RHIC energy $\sqrt{s} = 200$ GeV. We start our numerical computation at sufficiently high p_T (i.e. at early times τ_f) where the screening mass is small enough and the cross section is not screened in any significant way. At this p_T we then compute the screening mass $\mu_D^2(p_T)$ from Eq. 4 and with the obtained $\mu_D^2(p_T)$ we compute the screened cross section at $p_T - \Delta p_T$ (with a sufficiently small step Δp_T). From the resultant cross section we get the new screening mass at $p_T - \Delta p_T$ and so on. This iterative procedure gives us a self-consistent picture of screening: the bigger the cross section becomes the denser the parton medium gets and the larger a screening mass is generated, slowing down the rise of the cross section towards smaller p_T. In this way, the medium of produced minijets regulates the rapid growth of the jet cross section as seen in Fig. 3. Finally, at $\mu_D \sim p_T$, the cross section saturates. From Fig. 3 we see that for sufficiently large nuclei and for high collision energies this happens in the perturbative region $p_T \gg \Lambda_{QCD}$. To study the sensitivity of the results to the uncertainty relation (1), we show curves corresponding to $a = 1$ and $a = 2$. Note that due to the self-consistent iteration procedure the resulting difference in μ_D is not a trivial multiplicative factor $\sqrt{2}$.

In the computation we have used the MRSA parton distributions $f_i(x, Q)$ with a scale choice $Q = p_T$ [13]. At this point it is worthwhile to note that the singular parton distributions are stable against scale evolution, and the small-x growth $xf_i \sim x^{-\delta}$ persists even when going down to scales $p_T < 2$ GeV. Most of the cross section of Eq. 3 at fixed p_T comes from momentum fractions $x \sim 2p_T/\sqrt{s}$, so that a smaller scale p_T also corresponds to a smaller x. Therefore, when going towards smaller p_T, there is a competition between the scale evolution (causing a decrease in the parton density) and the small-x rise. As a result, the parton luminosity does not decrease fast enough to cancel the divergence in the $\hat{t}$- and $\hat{u}$-channels at small p_T. This is basically the reason for the rapid growth of the non-screened cross sections as seen in Fig. 3.

In the top panel of Fig. 4 we show the average number of produced minijets with $p_T \geq p_0$ and $|y| \leq 0.5$ in a central AA collision with $A = 200$. The curves are shown as functions of p_0 and they are obtained simply by integrating the cross sections in Fig. 3 over p_T from p_0 upwards and multiplying by $T_{AA}(\mathbf{0})$. The average transverse energy carried by these partons is obtained by weighting the cross sections of Fig. 3 by p_T and integrating again over p_T in the region $p_0 \leq p_T \leq \sqrt{s}/2$. The corresponding curves are shown in the lower panel of Fig. 4 as functions of p_0. Note also that p_0 here gives the time for formation of the system according to Eq. 1.

We want to point out how the parameter p_0 is needed as a cut-off only for the unscreened cross section. This cut-off makes the unscreened minijet production finite but the results depend strongly on the cut-off, as seen in Fig. 4. When the self-consistent screening is included the cross section saturates and there is no need for such a cut-off anymore, provided that the saturation occurs in the perturbative region

as it does in Fig. 3. However, one may still ask how many minijets are produced into the central rapidity unit with transverse momentum larger than some lower limit p_0, and what is the average transverse energy from these quanta. Fig. 4 gives an answer to these questions. Especially at the LHC energies, where the number of produced minijets becomes very large, and the parton system very dense, the average transverse energy practically saturates near $p_0 \sim 1$ GeV.

The weaker p_0-dependence should also make the perturbative energy density estimates of the early minijet system at $\tau_f(p_0) = a/p_0$ more reliable. In Fig. 5 the transverse energy density [14]

$$\varepsilon = \frac{\bar{E}_T^{AA}(p_0)}{\pi R_A^2 \tau_f(p_0) Y} \tag{5}$$

is plotted against p_0. Also the corresponding formation time is shown simultaneously. It is interesting to notice how the maximum energy density is reached at earlier times, and how the expansion of the system starts to dominate the evolution earlier when screening is taken into account. One should, however, keep in mind that the finite overlap of the colliding nuclei will reduce the energy density estimates especially at RHIC energies [15]. On the other hand, roughly half of the released final transverse energy is expected to originate from the soft particle production at RHIC energies [4,5,15]. This will slow down the decrease in ε at a later stage [15].

The screening effect we discussed here is due to final state interactions of produced partons. We should point out that there will also be screening effects, coming from initial state interactions or the color confining radius in the dense parton clouds of a high energy nucleus [16]. Ideally, one should take into account both screening effects in the calculation of parton production. Nuclear shadowing due to initial-state interactions will also reduce the estimates on semihard parton production especially at the LHC nuclear collisions, perhaps even at RHIC energies [5,17]. Nuclear gluon distributions are still uncertain to a large extent, and especially the scale dependence of nuclear gluon shadowing has to be studied carefully, e.g., as done in [17], but with the modern parton distributions like used in this paper [18].

In summary, we have considered color screening of initial semihard parton production in a phenomenological but self-consistent manner. Following Ref. [7] we have computed the static electric screening mass of the parton system by using the number distributions of produced minijets and by taking into account the formation time of the minijets. We do not try to estimate the corresponding magnetic screening mass, instead we use the obtained electric screening mass as a regulator for the divergent t and u-channel sub-processes. We have iteratively computed the lowest order minijet cross section with a feedback from the screening mass towards the region $p_T \sim \mu_D \lesssim 2$ GeV. We have shown that for sufficiently large nuclei and for sufficiently large energies, we obtain saturation of the minijet cross section in the perturbative region $p_T \gg \Lambda_{QCD}$. From this we conclude that the average number of minijets in the

central rapidity unit is finite and, furthermore, there is no need for an *ad hoc* cut-off parameter p_0. However, the question of how many minijets are produced with $p_T \geq p_0$ is still quite valid, and we have shown that the answer depends on the lower limit p_0 much more weakly than when screening effects are neglected. In the estimates of perturbative transverse-energy production there is practically no p_0-dependence below $p_0 \lesssim 1$ GeV at the LHC energy. Finally, we have shown how much the screening reduces the Bjorken estimate of the energy density of the early parton plasma.

ACKNOWLEDGEMENTS

We thank the European Center for Theoretical Studies in Nuclear Physics and Related Areas in Trento (Italy) for warm hospitality and providing a stimulating environment for discussions. We also thank M. Gyulassy, H. Heiselberg, K. Kajantie, P.V. Ruuskanen and A. Schäfer for discussions. KJE thanks the Academy of Finland for financial support. This work was supported by the Director, Office of Energy Research, Office of Nuclear Physics, Divisions of Nuclear Physics of the U.S. Department of Energy under Contract grant No. DE-AC03-76SF00098, DE-FG05-90ER40592.

REFERENCES

[1] T.K. Gaisser and F. Halzen, Phys. Rev. Lett. **54**, 1754 (1985);
G. Pancheri and Y. N. Srivastava, Phys. Lett. **B182**, 199 (1986);
L. Durand and H. Pi, Phys. Rev. Lett. **58**, 303 (1987);
R.C. Hwa, Phys. Rev. D **37**, 1830 (1988).

[2] X.-N. Wang, Phys. Rev. **D43**, 104 (1991).

[3] J.P. Blaizot, A.H. Mueller, Nucl. Phys. **B289**, 847 (1987).

[4] K. Kajantie, P. V. Landshoff and J. Lindfors, Phys. Rev. Lett. **59**, 2517 (1987);
K.J. Eskola, K. Kajantie and J. Lindfors, Nucl. Phys. **B323**, 37 (1989).

[5] X.-N. Wang and M. Gyulassy, Phys. Rev. **D44**, 3501 (1991); *ibid.* **D45**, 844 (1992); Phys. Rev. Lett. **68**, 1480 (1992); Comp. Phys. Comm. **83**, 307 (1994).

[6] K. Geiger and B. Müller, Nucl. Phys. **B369**, 600 (1992);
K. Geiger, Phys. Rev. **D47**, 133 (1993).

[7] T.S. Biró, B. Müller and X.-N. Wang, Phys. Lett. **B283**, 171 (1992).

[8] S.D. Ellis, Z. Kunszt and D. E. Soper, Phys. Rev. Lett. **62**, 726 (1989);
Phys. Rev. **D40**, 2188 (1989); Phys. Rev. Lett. **69**, 1496 (1992);
Z. Kunszt and D. E. Soper, Phys. Rev. **D46**, 192 (1992).

[9] K.J. Eskola and X.-N. Wang, "High p_T Jet Production in pp Collisions", in *Hard Processes in Hadronic Interactions,* eds. H. Satz and X.-N. Wang, Int. J. Mod. Phys. **A10**, 2881 (1995).

[10] K.J. Eskola, K. Kajantie and P.V. Ruuskanen, Phys. Lett. **B332**, 191 (1994);
K.J. Eskola, in Proc. of *Quark Matter '95*, eds. A.M. Poskanzer *et al.*, Nucl. Phys. **A590**, 383c (1995).

[11] H.A. Weldon, Phys. Rev. **D26**, 1394 (1982).

[12] K. Kajantie and J. Kapusta, Ann. Phys. **160**, 477 (1985);
J. Kapusta, "Finite-Temperature Field Theory," Cambridge University Press 1989, p. 143.

[13] A. D. Martin, W. J. Stirling and R. G. Roberts, Phys. Rev. **D51**, 4756 (1995).

[14] J.D. Bjorken, Phys. Rev. **D27**, 140 (1983).

[15] K.J. Eskola and M. Gyulassy, Phys. Rev. **C47**, 2329 (1993).

[16] L. McLerran and R. Venugopalan, Phys. Rev. **D49**, 2233 (1994), *ibid.* **D50**, 2225 (1994).

[17] K.J. Eskola, Nucl. Phys. **B400**, 240 (1993).

[18] K.J. Eskola, J. Qiu and X.-N. Wang, work in progress.

FIGURES

FIG. 1. An example of a process contributing to the screening. Off-shell gluons are drawn in thick lines.

FIG. 2. Longitudinally boost invariant space-time picture of an AA collision. The z-axis is along the beam, and the longitudinal proper time is $\tau = \sqrt{t^2 - z^2}$. Partons in the central region within a rapidity interval Y (between the solid lines) and with transverse momenta $p_T > a/\tau_1$ have formed earlier than τ_1, and thus screen the formation of partons at $\tau \geq \tau_1$.

FIG. 3. (**a**) Differential minijet cross section $d\sigma_{\rm jet}/dp_T dy$ at $y = 0$ and screening mass μ_D as functions of transverse momentum p_T in a pp sub-process of a central AA collision at $\sqrt{s} = 5.5\,A$TeV with $A = 200$. The dashed line is for unscreened cross section, the solid and dotted curves for the screened case with different parameters a from Eq. 1. Nuclear shadowing is not taken into account. (**b**) The same as in panel (a) but for $\sqrt{s} = 200\,A$GeV.

FIG. 4. (**a**) The average number of minijets produced with $p_T \geq p_0$ and $|y| \leq 0.5$ in a central AA collision as a function of p_0 (see the text). The solid, dotted and dashed curves correspond to the curves in Fig. 3, and the two sets of curves are for energies $\sqrt{s} = 200$ and 5500 AGeV. (**b**) The average transverse energy of the minijets of panel (a) as a function of p_0 (see the text). Labeling of the curves is the same as in panel (a).

FIG. 5. Transverse energy density ε of the perturbatively produced minijet system as a function of the smallest transverse momentum p_0. The corresponding formation time axis is also shown. The upper set of curves is for $\sqrt{s} = 5500\,A$GeV and the lower set for $\sqrt{s} = 200\,A$GeV. The solid and dashed lines show the estimate with and without screening, respectively, for $a = 1$.

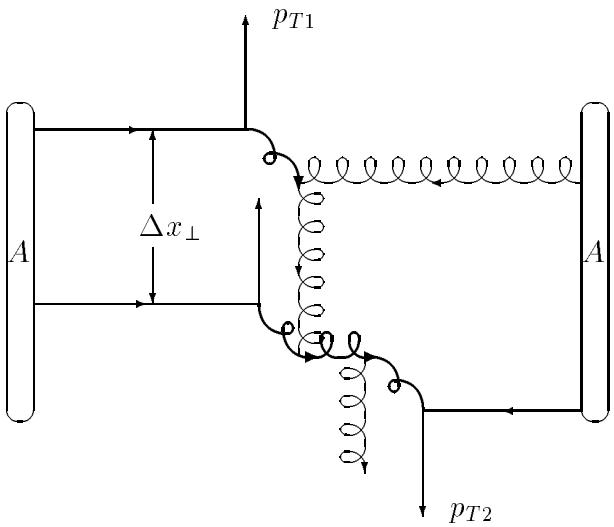

Fig. 1

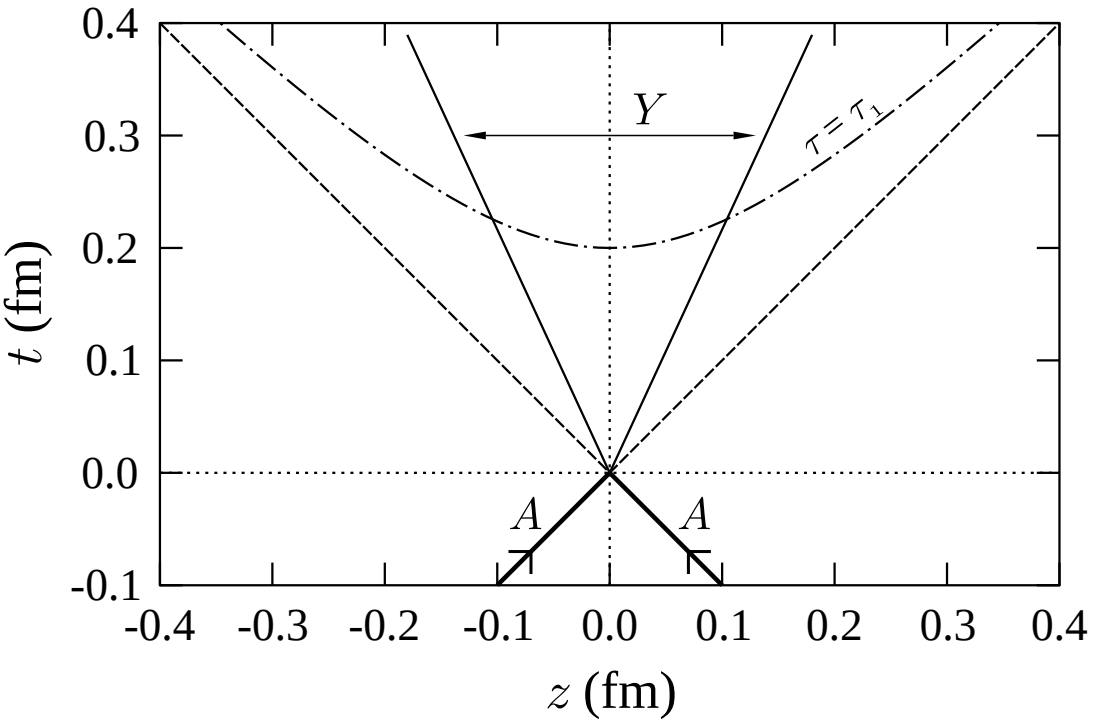

Fig. 2

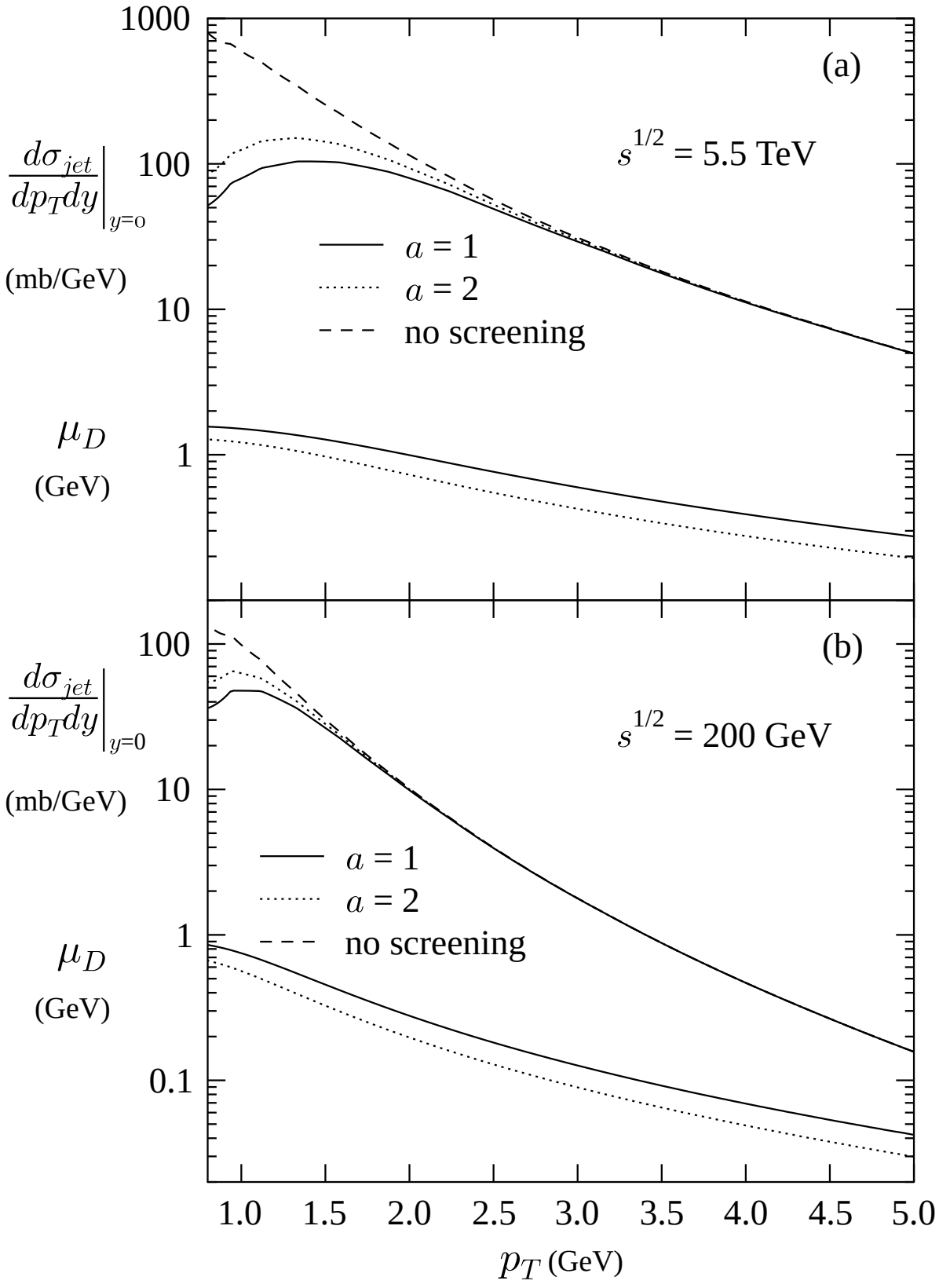
1000
100
10
1
0.1
(a)
(b)
$s^{1/2}$ = 5.5 TeV
$s^{1/2}$ = 200 GeV
a = 1
a = 2
no screening
$\frac{d\sigma_{jet}}{dp_T dy}\Big|_{y=0}$
(mb/GeV)
μ_D
(GeV)
1.0
1.5
2.0
2.5
3.0
3.5
4.0
4.5
5.0
p_T (GeV)

Fig. 3

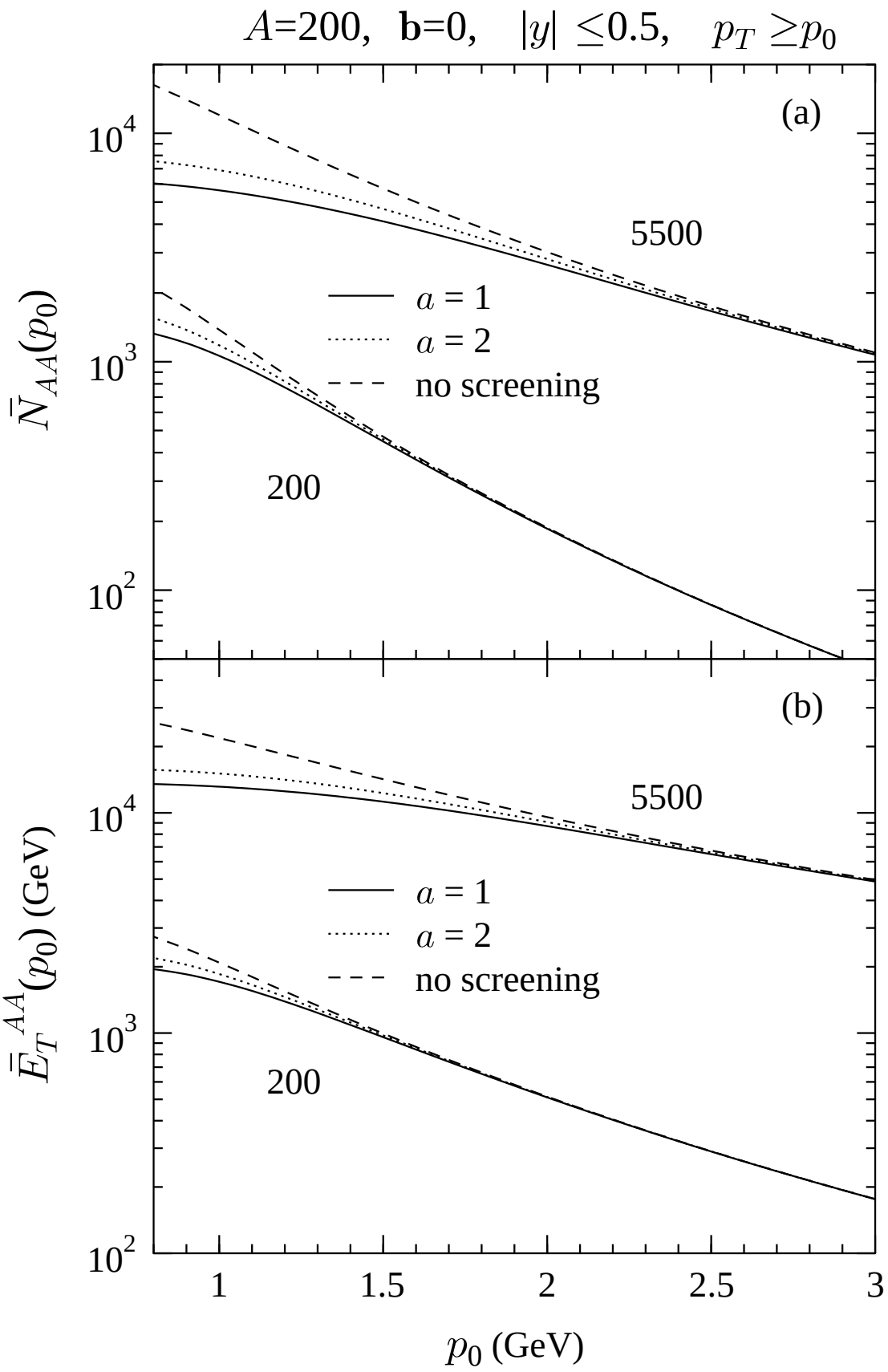
A=200, **b**=0, $|y| \leq 0.5$, $p_T \geq p_0$
(a)
5500
200
a = 1
a = 2
no screening
$\bar{N}_{AA}(p_0)$
(b)
5500
200
a = 1
a = 2
no screening
$\bar{E}_T^{AA}(p_0)$ (GeV)
10^4
10^3
10^2
1
1.5
2
2.5
3
p_0 (GeV)

Fig. 4

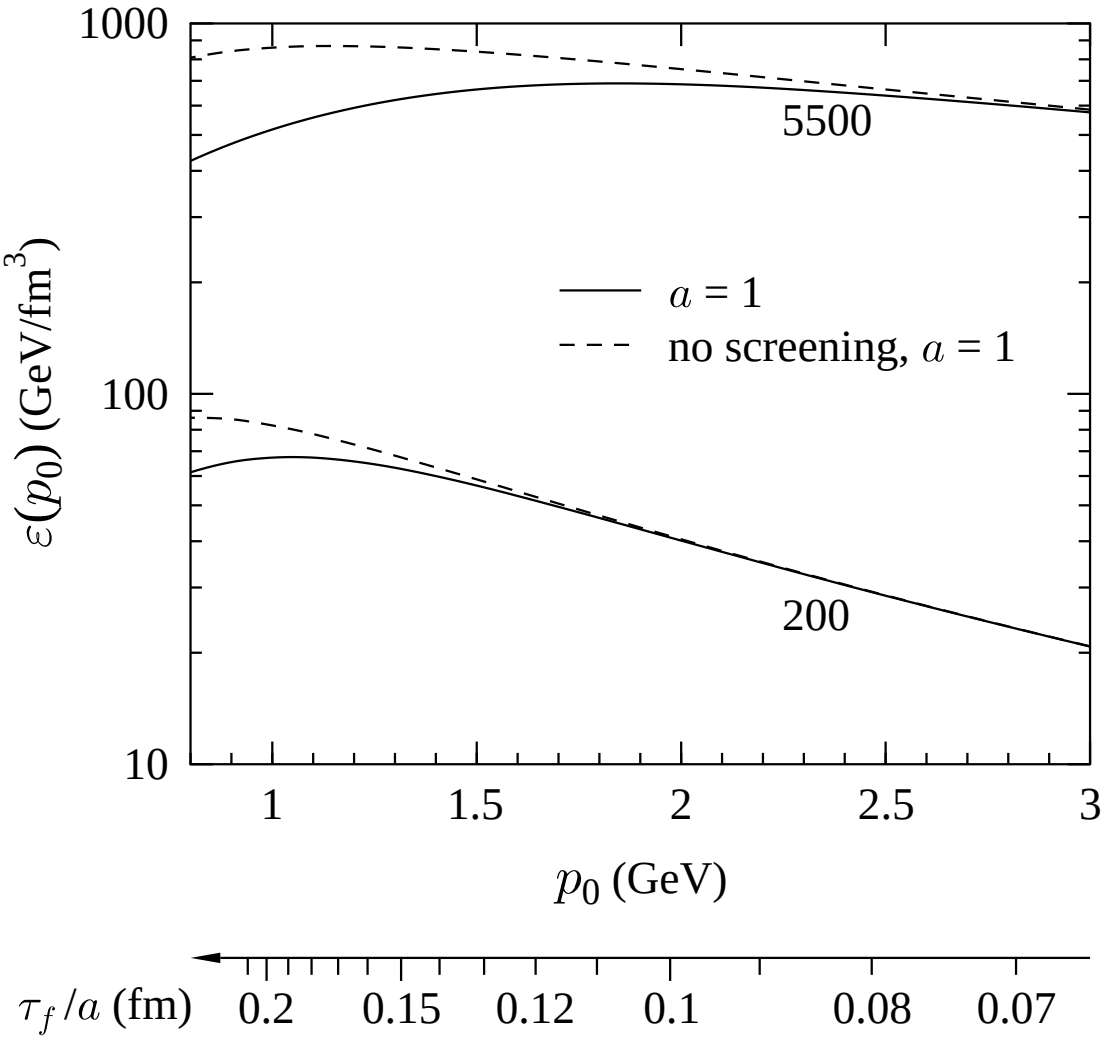
1000
100
10
$\varepsilon(p_0)$ (GeV/fm^3)
5500
200
a = 1
no screening, a = 1
1
1.5
2
2.5
3
p_0 (GeV)
τ_f/a (fm)
0.2
0.15
0.12
0.1
0.08
0.07

Fig. 5